



Joint planning for battery swap and supercharging networks with priority service queues

Jie Zhang^a, Lihui Bai^a, Tongdan Jin^{b,*}

^a Department of Industrial Engineering, University of Louisville, Louisville, KY, 40292, USA

^b Ingram School of Engineering, Texas State University, San Marcos, TX, 78666, USA

ARTICLE INFO

Keywords:

Battery swap
Supercharger
Erlang queue
Power grid reliability
Heuristic optimization
Location-allocation model

ABSTRACT

Existing network planning models for electric vehicle (EV) services usually treat the battery swap and the on-board supercharging as two independent processes. This study makes an early attempt to design an EV charging network where battery swap and supercharging are jointly coordinated. The swap and supercharge processes are characterized by Erlang B and Erlang C priority queues, respectively. A strategic location-allocation model is formulated to optimize the station sites, battery stock level, and the number of superchargers at chosen sites. Three design criteria, namely, battery state-of-charge, maximum service time, and power grid constraint, are simultaneously taken into account. Meta-heuristics algorithms incorporating Tabu search are developed to tackle the proposed non-linear mixed integer optimization model. Computational results on randomly generated instances show that the priority battery service scheme outperforms the pure battery swap station in terms of spare battery investment cost and charging flexibility. The case study on a real-world traffic network comprised of 0.714 million households further shows the efficacy and advantage of the dual battery charging process for ensuring state-of-charge, service time commitment, and network-wide grid stability.

1. Introduction

There exist several obstacles against the mass adoption of electrical vehicles (EV). Unlike gasoline cars, EV requires much longer time and sophisticated equipment to recharge the battery. In addition, the number of EV chargers in public places such as parking lots, office buildings, shopping malls, and rest areas of highways, is still far less compared to gas stations. Therefore, battery recharging time, range anxiety, and limited service accessibility are the main hurdles to mass EV adoption.

Pure battery swap station (PBSS) allows EVs to replace a depleted battery with a fully charged unit (i.e. spare battery) in minutes. The station then moves those depleted batteries into the charge bay where they are recharged. Upon recharging, the same battery can be reused for future incoming EV. In 2013, Tesla demonstrated the concept of PBSS at a ready-for-implementation scale (Byford, 2013). The Tesla station completes the swap process in just 90 s, even faster than refueling a gas tank for conventional cars. In 2016, BJEV, a subsidiary of Beijing Automotive Group, established 50 battery swap and charging stations to serve the needs of at least 6000 EV taxis (Li, 2016). In this business model, batteries are owned by the PBSS and leased to EV drivers. This significantly lowers the EV selling price because a single battery pack

usually accounts for one-third of a vehicle cost (Agassi, 2009). In the meantime, the PBSS can bill EV drivers based on the battery energy usage, instead of its capital cost (Avci et al., 2015). Such a business model can also help to alleviate EV owners' concern with battery reliability and performance degradations because these issues can be undertaken by the PBSS.

In this paper we propose to deploy an EV battery service infrastructure with a dual charging mode. The first is the pure battery swap station (PBSS) that only offers battery exchange services. When an EV arrives at a PBSS, the depleted battery is replaced with a spare item that has been charged to a required state-of-charge (SOC) level (e.g., 95%). If a spare battery is not available, the EV has to wait until a read-for-use battery is available from the charge bay. The second infrastructure is called joint battery swap and supercharging (JBSS) station that provides battery exchange and onboard fast charging in the same facility. When an EV arrives at a JBSS station, the default option is the battery swap. If the station is out of spare batteries, the EV will use the onsite supercharger to recharge its onboard battery. For example, a 24 kWh battery of a Nissan Leaf can be fully recharged in approximately 10 min using 150 kW. If the battery swap is the only service option, under high demand pressure spare batteries with low SOC may be used to reduce the

* Corresponding author.

E-mail address: tj17@txstate.edu (T. Jin).

<https://doi.org/10.1016/j.ijpe.2020.108009>

Received 20 March 2020; Received in revised form 14 October 2020; Accepted 17 December 2020

Available online 24 December 2020

0925-5273/© 2020 Elsevier B.V. All rights reserved.

waiting time for an EV. In contrast, JBSS ensures that a spare battery always meets the required SOC level prior to the use.

Given the potential advantages of the dual battery charging stations, we further examine the logistical and operational aspects of a JBSS network. First, EV travel patterns and demand profiles may vary in a given area. This requires service stations to be properly located in view of the observed traffic pattern. Second, each station also needs to determine the proper amounts of spare batteries and superchargers so as to lower the capital cost. For instance, a 24 kWh lithium-ion battery pack would cost \$7200 and the cost of a 40 kWh battery exceeds \$12,000. Third, it is worth considering the costs of other equipment, such as charge bays and auxiliary devices, at each station. Establishing a PBSS station typically costs \$0.5 to \$1 million (Fang et al., 2017). To balance the service quality and the cost effectiveness, a holistic approach is needed for the planning and operation of EV service networks.

The contribution of this paper is three-fold. First, to the best of our knowledge, this work is the first attempt to investigate a location-allocation model considering both battery swap and onboard supercharging with priority services. We jointly optimize the station site, the spare battery stock, and the number of superchargers for minimizing the infrastructure cost. Second, the operation of a JBSS station is characterized as a two-stage priority queue formed by Erlang B and C in tandem, and the swapping is precedent to the supercharging. Third, we consider the demand uncertainty, range anxiety, and charging time variations. The proposed planning model is able to achieve three performance goals: guaranteed battery SOC level, ensured customer service time, and controlled load to the power grid. In addition, we developed a Tabu search algorithm that can efficiently search for the optimal or near-optimal solution.

The remainder of the paper is organized as follows. Section 2 reviews the literature on EV service stations and network design. Section 3 presents a two-stage Erlang priority queue for modeling JBSS operations. Subsequently, two planning models pertaining to PBSS and JBSS are formulated. Section 4 presents the Tabu search algorithm for solving both models. Sections 5 and 6 perform numerical experiments and case study, and managerial insights are derived. Section 7 concludes the paper.

2. Literature review

The literature pertaining to EV battery service station planning can be classified into three categories: 1) vehicle-to-grid (V2G) and grid-to-vehicle (G2V) operations; 2) service analysis and performance optimization of a single PBSS; and 3) location and allocation of PBSS networks. Below we review these related works.

The first research stream analyzes the impact of PBSS on the power grid under V2G or G2V schemes. Pan et al. (2010) formulate a two-stage stochastic programming model to locate the PBSS sites and allocate the battery stock level in each station to meet a power demand with V2G operation. In their model, the EV arrival is treated as a deterministic process with a fixed rate. Armstrong et al. (2013) study the PBSS operating strategy in a day-ahead market with V2G and G2V decisions. They compute the optimal electricity prices and volumes to be transacted in the market to maximize the revenue. Widrick et al. (2016) tackle a PBSS management problem to determine the optimal policy for V2G and G2V that maximizes the total profit over a fixed time horizon. Ren et al. (2019) use a graph convolutional neural network to predict EV demand at the station level. A dynamic pricing scheme considering vehicle relocation cost and V2G revenue is used to maximize the total revenue from EV sharing network. Kabli et al. (2020) propose a two-stage stochastic program to determine a power grid expansion in conjunction with EV charging station siting. The first stage identifies the locations to expend power grid and the second stage sites the charging stations for total cost minimization. Liu et al. (2020) use a fuzzy multi-criteria decision-making to select charging station locations for EV fleet. The method first uses the Delphi method to determine the station locations

and further applies fuzzy grey relation analysis to derive the weights for the design criteria such as cost and service time. Our model also incorporates the electricity transaction criteria into the daily station operation. The main difference is that in our model the grid power capacity, the battery SOC level, and the customer service time are simultaneously considered.

The second research stream aims at optimizing the performance of a single PBSS station in the presence of demand uncertainty. Yudai and Osamu (2009) divide the battery recharge process into three phases: waiting, under recharging, and fully charged. A queueing model is used to calculate the number of batteries a station should hold to meet the pre-defined service level. Raviv (2012) schedules the charging process in a PBSS station with the objective of optimizing a weighted measure of service quality and penalty cost. It shows that first-come-first-served (FIFO) results in less penalty cost under fixed charge capacity and float price. Liu (2015) proposes a service index called "availability of battery swapping service per day" (ABSSD), to evaluate the performance of a single station powered by onsite photovoltaics. ABSSD represents the percentage of vehicles that obtain a fully charged battery in a day. Tan et al. (2018) model the battery swap process as a Markov chain and a steady state probability is used to determine the risk of blocked EV. Our work resembles these studies in that we also use queueing models to establish the relation between the battery stockout rate and the expected service time. The main difference is that we construct a two-stage queueing network to prioritize the battery swap over the supercharging process, whereas they are often handled singularly in existing literature.

The third research stream focuses on the infrastructure design by siting the stations and sizing the battery stock to meet the service level requirement with low cost. Assuming the battery stock is known, Wang and Lin (2009) propose an integer programming model to optimize the number of PBSS sites using the actual traffic flows of the origin-destination pairs. Mak et al. (2013) propose a quadratic optimization model to locate the station sites and further allocate the battery inventory such that the total infrastructure cost is minimized. A combination of FIFO policy and recharge duration is used to manage the battery SOC. Jamian et al. (2014) use an artificial bee colony algorithm to search for the optimal siting and sizing of battery swap stations by minimizing the total power loss. Since PBSS location-allocation problem is a complex capacity decision-making process, relaxation techniques and heuristic algorithms are often used to tackle this type of problem (Eiselt and Sandblom, 2013; Tran et al., 2018). Our work also investigates the station location-allocation problem with two distinctive aspects. First, we incorporate superchargers into the classical location-allocation model. This dual service mode allows an EV to recharge the onboard battery if the stock is out of spare battery. Second, using superchargers allows the station to guarantee the battery SOC in charge bays. This is a main advantage over existing models where in order to reduce waiting time, spare batteries with an unsatisfactory SOC level may be used.

It is worth mentioning that EV service infrastructure planning is closely related to facility location-allocation models that have been investigated in operations management community (Drezner and Hamacher, 2001). For instance, Shen and Qi (2007) study the number and locations of distribution centers facing normally distributed demands. Lagrangian relaxation embedded with a branch-and-bound algorithm is used to minimize the objective function comprised of location, inventory, and routing costs. Later Mak and Shen (2009) investigate a two-echelon inventory-location problem under a Poisson demand process. Diabat et al. (2017) solve a joint inventory-location problem by considering customer demand as a Markov process and compute the expected reorders, lost sales, and inventory based on queueing theory. The problem is solved by using simulated annealing and a direct search method. A main difference is that our model not only meets the random customer demand, but also ensures the power grid stability with the coordination of two priority service queues.

3. Two-stage queueing for battery swap and supercharging

3.1. The operation of a JBSS station

Fig. 1 describes the working principle of a JBSS station that provides battery swap and onboard supercharging services. When an EV arrives at a station with a depleted battery, the battery is replaced with a spare item if available. Otherwise the EV is moved to the supercharger area for onboard battery charging. When an EV leaves the JBSS, either the depleted battery is exchanged, or its own battery is recharged via supercharger. Thus, a JBSS station can be treated as a priority queueing network comprised of a swap queue followed by a supercharge queue. Below the characteristics of this priority queue is discussed in detail.

Vehicle Arrivals: Two assumptions are made regarding the EV arrival process. First, EV arrivals at a JBSS occur independently and randomly. Second, the arrival rate is a constant. These two assumptions allow us to model the arrival stream as a Poisson process, which also has been used in the literature, for example Mak et al. (2013), Tan et al. (2014), and Avci et al. (2015).

Charging Duration: The charging duration, also known as charging cycle time, is defined as the elapsed time by recharging a depleted battery to a desired SOC level. Charging duration may vary significantly because the energy residuals of batteries unloaded from EV differ from each other. Hence a general distribution is more appropriate to describe the charging time. In addition, given two identical batteries with the same energy residual, the charging duration also differs depending on the level of charging power (Voelcker, 2018).

Battery Stock: The battery stock level is a decision variable and plays a critical role in achieving the required service level. In JBSS model, an incoming EV receives the swap service only if a spare battery with required SOC level is available; otherwise, the EV turns to superchargers.

Superchargers: The number of superchargers in a station is also a decision variable. High equipment cost coupled with power grid capacity limit precludes a large amount of supercharger installation at a station. For example, a Tesla’s supercharging station typically has 5–7 superchargers (Lambert, 2017). Hence, a waiting queue may be created in supercharging.

Based on these discussions, the battery swap process can be modeled as an $M/G/s/s$ Erlang B queue with customer blocked, and s is the spare battery stock level. Similarly, the supercharging process can be modeled as an $M/M/m/\infty$ Erlang C queue with m being the number of superchargers. While Erlang B has no waiting line, Erlang C allows EV to wait if all superchargers are occupied. Both Erlang B and C models have been applied in a variety of fields where similar queueing patterns exhibit, such as inventory management (Bijvank and Johansen, 2012), single server effect (Liu and Kulkarni, 2008), and clinical planning (Bekker and de Bruin, 2009). Table 1 lists the notation and parameters in the

Table 1
Parameters and decision variables.

i	Index of customer zone, for $i = 1, 2, \dots, I$
j	Index of candidate station location, for $j = 1, 2, \dots, J$
d_{ij}	Indicate whether station j is within half battery range of customer zone i
γ	The probability of being blocked in battery swap queue
β	The probability of waiting in supercharging queue
λ_b	EV arrival rate of a station
λ_d	EV arrival rate for supercharging service in a station
μ_b	Battery recharge rate of a charge bay
μ_d	Supercharging rate
θ	EV arrivals during a charging cycle of charge bay (i.e., $1/\mu_b$)
φ	EV arrivals during a supercharging cycle (i.e., $1/\mu_d$)
τ_b	Duration for swapping a battery given the spare is ready
$B(s)$	Probability of spare battery stockout
$C(m)$	Probability that an EV waits for a supercharger
F_j	Setup cost for station j
F_b	Unit cost of spare battery
F_d	Unit cost of supercharger
N_b	The expected number of batteries in the charge bay under recharging
N_q	The expected number of EV waiting for superchargers
N_c	The expected number of EV under supercharging
N_d	Total number of EV in supercharging, and $N_d = N_q + N_c$
P_b	Level of charging power in a charge bay
P_d	Level of supercharging power of a supercharger
P_j	Power grid capacity of station j
W_q	Waiting time of an EV in a supercharge queue
W_c	The actual time for supercharging an EV battery
W	Total service time in battery supercharging, $W = W_q + W_c$
W_{max}	Pre-specified service time limit for an EV
Decision Variables	
x_j	Whether a station opens in location j , binary variable
y_{ij}	Whether station j covers zone i , binary variable
s_j	The amount of spare batteries allocated in station j , integer variable
m_j	The number of superchargers installed in station j , integer variable

subsequent presentation.

3.2. Battery swap queue

To simplify the notation, the subscript of s and m is omitted in the following derivation because both are associated with a particular station. Let $k = 0, 1, \dots, s$ be the number of batteries under recharging in the charge bays of a station. Assume abundant charge bays are available. The battery swap process with EV blocked is modeled as $M/G/s/s$ queue, and its transition diagram is shown in Fig. 2 below.

Note that λ_b is the EV arrival rate (e.g. cars/hour), and μ_b is the battery recharge rate in the charge bay. Namely, to charge a depleted battery to the desired SOC level, the average time duration is $1/\mu_b$. Given the battery base stock level s , the probability that an incoming EV is blocked in the swap queue, denoted as $B(s)$, can be estimated as follows,

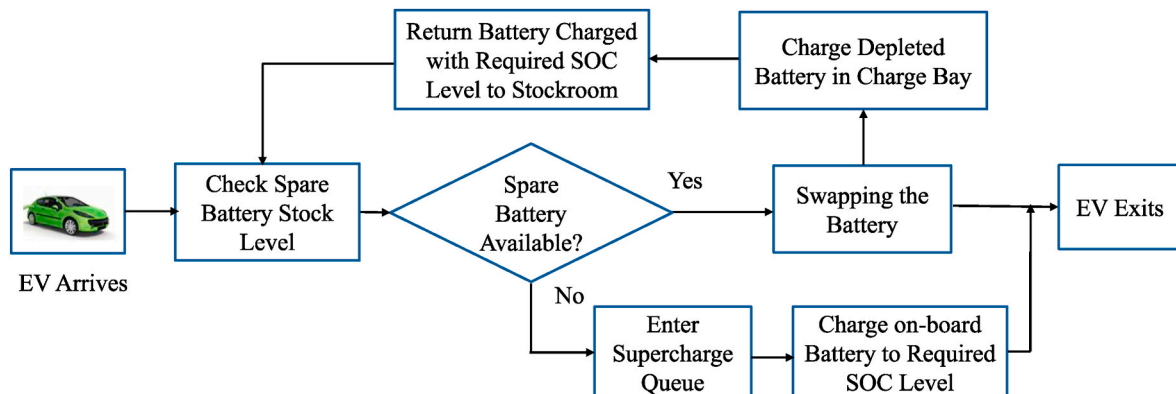


Fig. 1. Joint battery swap and supercharge station with priority queue.

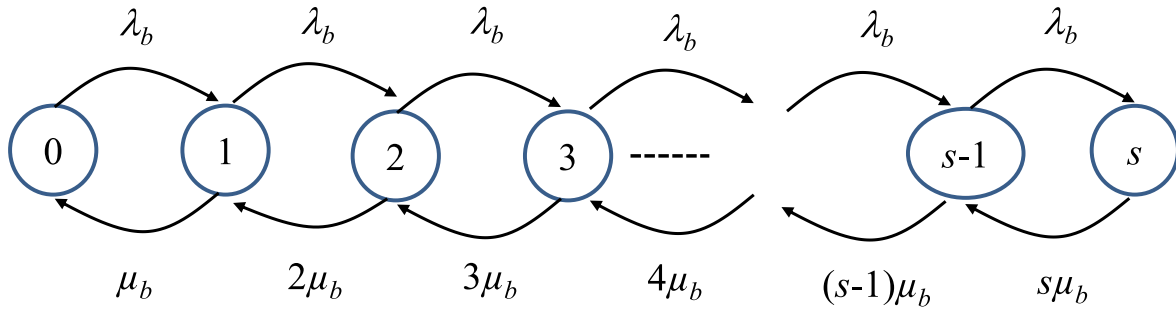


Fig. 2. The M/G/s/s queue for battery swap.

$$B(s) = \frac{\frac{(\lambda_b/\mu_b)^s}{s!}}{\sum_{k=0}^s \frac{(\lambda_b/\mu_b)^k}{k!}} = \frac{\theta^s}{s!} \frac{1}{\sum_{k=0}^s \frac{\theta^k}{k!}} \quad (1)$$

Equation (1) is also known as the Erlang loss function or Erlang B formula (Winston, 2004). Note that $\theta = \lambda_b/\mu_b$ is called the offered load, representing the average number of arriving vehicles during $1/\mu_b$. If N_b is the number of batteries under recharging in the charge bay, then

$$E[N_b] = \frac{\lambda_b}{\mu_b} (1 - B(s)) = \theta(1 - B(s)) \quad (2)$$

Equation (2) allows us to estimate the power demand of the charge bay, which will be discussed in Section 3.4. Below we briefly review several important properties of $B(s)$.

Lemma 1. (Zeng, 2003) Erlang loss function can be calculated by its inverse to ensure numerical stability. Namely:

$$B(\theta, s) = \begin{cases} 1 & \text{for } s = 0 \\ \frac{1}{1 + R(\theta, s - 1)\theta/s}, & \text{for } s = 1, 2, 3, \dots \end{cases}$$

Lemma 2. (Whitt 1992) Erlang queueing function can be calculated by inverse function of Erlang loss function to ensure numerical stability, namely,

$$E(\theta, s) = \frac{1}{R(\theta, s) - R(\theta, s - 1)}.$$

Lemma 3. (Whitt 1992) $B(\theta, s)$ and $E(\theta, s)$ monotonically increase with θ .

Lemma 4. (Whitt 1992) $B(\theta, s)$ and $E(\theta, s)$ monotonically decrease with s .

Mathematical properties stated in Lemmas 1-4 are important to design the metaheuristic algorithms in Section 4. In particular, Lemma 1 provides a practical approach to computing $B(s)$ because explicit calculation of the factorials poses a computational challenge when s is large. Lemmas 2-4 describe the relations among EV arrival rate, battery stock, and service level.

3.3. Supercharging queue

An arrived EV is redirected to the supercharging queue if all spare batteries run out. A supercharger uses the DC fast charging technology with output power up to 150 kW based on Tesla standards (Wikipedia, 2020). Let λ_d be the EV arrival rate of the supercharging queue, then.

$$\lambda_d = \lambda_b B(s) \quad (3)$$

The above result is due to the fact that all EV blocked in the swap queue receive the supercharging service. Since $0 < B(s) \leq 1$, we have $\lambda_d \leq \lambda_b$. Fig. 3 depicts the transition diagram of M/M/m/∞ queue where m is the number of superchargers in the station.

Note that μ_d is the service rate per supercharger (e.g. EV/hour), or equally $1/\mu_d$ is the average supercharging duration. The M/M/m/∞ system is also referred to as the Erlang C delayed model because it accommodates a waiting line when all superchargers are busy. Denoted as $C(m)$, the probability that an EV needs to wait is given as (Winston, 2004):

$$C(m) = \frac{\frac{\varphi^m}{m!(1-\varphi/m)}}{\sum_{k=0}^{m-1} \frac{\varphi^k}{k!} + \frac{\varphi^m}{m!(1-\varphi/m)}} = \frac{\frac{(m\rho_d)^m}{m!(1-\rho_d)}}{\sum_{k=0}^{m-1} \frac{(m\rho_d)^k}{k!} + \frac{(m\rho_d)^m}{m!(1-\rho_d)}}, \quad (4)$$

where $\varphi = \lambda_d/\mu_d$ represents the offered rate, and $\rho_d = \lambda_d/(m\mu_d)$ is called the traffic intensity rate. The Erlang C queue is stable only if $\rho_d < 1$. Equation (3) indicates that λ_d is a function of λ_b and $B(s)$, hence we have

$$\rho_d = \frac{\lambda_b}{m\mu_d} B(s). \quad (5)$$

Substituting Equation (5) into Equation (4) yields

$$C(m, s) = \frac{\frac{(B(s)\lambda_b/\mu_d)^m}{m!(1-B(s)\lambda_b/(m\mu_d))}}{\sum_{k=0}^{m-1} \frac{(B(s)\lambda_b/\mu_d)^k}{k!} + \frac{(B(s)\lambda_b/\mu_d)^m}{m!(1-B(s)\lambda_b/(m\mu_d))}}. \quad (6)$$

Intuitively, larger m and s imply a smaller probability that an EV needs to wait for a supercharger. Let N_q be number of the EV in waiting, and N_c be those under supercharging. Then we have

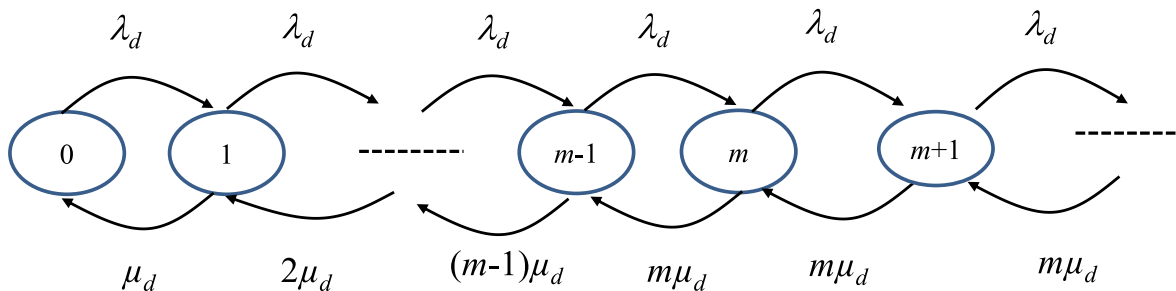


Fig. 3. The M/M/m/∞ queue for supercharging service.

$$E[N_q] = \frac{\rho_d C(m, s)}{1 - \rho_d} = \frac{\lambda_b B(s) C(m, s)}{m\mu_d - \lambda_b B(s)}, \quad (7)$$

$$E[N_c] = \frac{\lambda_d}{\mu_d} = \frac{\lambda_b B(s)}{\mu_d}. \quad (8)$$

Thus, the total EV in the supercharging queue, denoted as $E[N_d]$, is obtained as

$$E[N_d] = E[N_q] + E[N_c] = \frac{\lambda_b B(s) C(m, s)}{m\mu_d - \lambda_b B(s)} + \frac{\lambda_b}{\mu_d} B(s) \quad (9)$$

Finally, the total service time in the supercharging queue, denoted as W , is given as

$$W = W_q + W_c = \frac{C(m, s)}{m\mu_d - \lambda_d} + \frac{1}{\mu_d} \quad (10)$$

Where W_q and W_c represent the waiting time and the actual supercharging time, respectively. A distinction shall be made between μ_b in Equation (1) and μ_d in Equation (10). The former is the battery recharging rate in the charge bay, and the latter is the supercharging rate. To preserve the battery life, medium voltage and power can be used in the charge bay. For instance, adopting Level-2 charger with 220 V can recharge a 24 kWh battery in 4 h or $\mu_b = 0.25$ battery/hour as opposed to 0.5 h using Level-3 charger or $\mu_d = 2$ battery/hour (SAE, 2010). Tesla maintains its own charge standards and its supercharger can deliver up to 150 kW as opposed to 80 kW of Level-3 charger.

3.4. PBSS network planning model

First we formulate a PBSS location-allocation model based on Erlang C queue because an arriving EV with depleted battery has to exchange the battery even if the inventory is out of stock. Let I be the number of customer zones and J be the number of candidate station locations. Without loss of generality, we assume customers opt to use a PBSS only if the distance between the PBSS and customers is less than 50% of battery drive range. A binary parameter d_{ij} is introduced to indicate whether a PBSS is within half battery range of a customer zone for $i = 1, 2, \dots, I$, and $j = 1, 2, \dots, J$. EV arrives at a PBSS according to the Poisson process with rate λ_i . The model decides where a station should be opened, which customer zone(s) are assigned to the opened station, and how many spare batteries should be allocated at the station. The goal is to minimize the total cost for opening stations subject to the service time requirement. The optimal PBSS Location (PBSSL) model is formulated as follows:

PBSSL Model:

$$\text{Min} : f(\mathbf{x}, \mathbf{s}) = \sum_{j=1}^J (F_j x_j + F_b s_j) \quad (11)$$

Subject to:

$$\sum_{j=1}^J y_{ij} = 1, \quad \text{for } \forall i \quad (12)$$

$$y_{ij} \leq d_{ij} x_j, \quad \text{for } \forall i \text{ and } j \quad (13)$$

$$\rho_j = \lambda_j / (s_j \mu_b) \quad \text{for } \forall j \quad (14)$$

$$\lambda_j = \sum_{i=1}^I y_{ij} \lambda_i, \quad \text{for } \forall j \quad (15)$$

$$\frac{C_j(s_j)}{s_j \mu_b - \lambda_j} + \frac{1}{\mu_b} \leq W_{\max}, \quad \text{for } \forall j \quad (16)$$

$$\frac{(s_j \rho_j)^s}{s_j! (1 - \rho_j)} \times \frac{1}{\sum_{k=0}^{s_j-1} \frac{(s_j \rho_j)^k}{k!} + \frac{(s_j \rho_j)^{s_j}}{s_j! (1 - \rho_j)}} = C_j(s_j), \quad \text{for } \forall j \quad (17)$$

$$s_j \rho_j P_b \leq P_j, \quad \text{for } \forall j \quad (18)$$

$$s_j \leq M x_j, \quad \text{for } \forall j \quad (19)$$

$$s_j \geq 0, \quad \text{for } \forall j \quad (20)$$

$$s_j \in Z, \quad \text{for } \forall j \quad (21)$$

$$x_j \in \{0, 1\}, \quad \text{for } \forall j \quad (22)$$

$$y_{ij} \in \{0, 1\}, \quad \text{for } \forall i \text{ and } j \quad (23)$$

The objective function (11) consists of the cost for setting up the stations and purchasing the spare batteries. Here x_j is the binary decision variable, and $x_j = 1$ indicates to open a station in location j , and not if $x_j = 0$. Also, s_j represents the number of spare batteries allocated in station j . Constraint (12) states that each customer zone must be assigned to one PBSS. Constraint (13) sets the maximum allowed distance (e.g., 50% of drive range of an EV) from a customer zone to the assigned PBSS. Constraint (14) calculates maximum possible service rate in Erlang C queue, and ρ_j is the traffic intensity rate of station j . Constraint (15) aggregates the EV arrival rate at a PBSS over all assigned customer zones. Constraint (16) ensures the total service time at station j does not exceed the pre-defined W_{\max} . Constraint (17) is the Erlang C queueing formula calculating the probability of battery stockout. Constraint (18) states that the power load of any station should not exceed the grid capacity. Note that P_b is the charging power in a charge bay. Constraint (19) ensures that no spare battery is allocated to a station unless the station opens. Constraints (20)-(23) specify the types of decision variables for s_j , x_j and y_{ij} , respectively.

3.5. JBSS network planning model

Next we present a network design model in which each station offers both battery swap and supercharging services. The former is characterized by Erlang B queue and the latter is modeled as an Erlang C queue. The swapping is in precedence to supercharging. The JBSS Location (JBSSL) model aims to minimize the total infrastructure cost subject to grid capacity and service time constraints.

JBSSL Model:

$$\text{Min} : f(\mathbf{x}, \mathbf{s}, \mathbf{m}) = \sum_{j=1}^J (F_j x_j + F_b s_j + F_d m_j) \quad (24)$$

Subject to:

$$\frac{\theta_j^{s_j} / s_j!}{\sum_{k=0}^{s_j} (\theta_j^k / k!)} = B_j(s_j), \quad \text{for } \forall j \quad (25)$$

$$\phi_j = B_j(s_j) \lambda_j / \mu_d, \quad \text{for } \forall j \quad (26)$$

$$\tau_b (1 - B_j(s_j)) + W_j \times B_j(s_j) \leq W_{\max}, \quad \text{for } \forall j \quad (27)$$

$$\frac{\frac{\phi_j^{m_j}}{m_j! (1 - \phi_j / m_j)}}{\sum_{k=0}^{m_j-1} \frac{\phi_j^k}{k!} + \frac{\phi_j^{m_j}}{m_j! (1 - \phi_j / m_j)}} = C_j(m_j, s_j), \quad \text{for } \forall j \quad (28)$$

$$(1 - B_j(s_j)) \theta_j P_b + \phi_j P_d \leq P_j, \quad \text{for } \forall j \quad (29)$$

$$m_j \geq 0, \quad \text{for } \forall j \quad (30)$$

$$m_j \in \mathbb{Z}, \quad \text{for } \forall j \tag{31}$$

Constraints (12)-(17) and (19)-(23)

The objective function (24) is the sum of the costs for station setup, battery purchase, and supercharger installation. The new decision variable m_j represents the number of superchargers in station j . Constraint (25) is the Erlang loss function, and θ_j is the number of EV arriving at station j during $1/\mu_b$. Constraint (26) calculates the average number of arrived EV during a supercharging cycle. Constraint (27) states that the total service time in a JBSS station must not exceed W_{\max} . With probability $1-B_j(s_j)$, the service time is τ_b by battery swap. With probability $B_j(s_j)$, the service time consists of waiting and actual supercharging time shown in Equation (10). Constraint (28) is the Erlang C formula calculating the waiting probability, and φ_j is the number of EV requesting supercharging in station j during $1/\mu_d$. Constraint (29) states that the total power demand of a PBSS station should not exceed the grid capacity. The station power demand consists of the load of charge bays and superchargers. Constraints (30) and (31) mandates m be a non-negative integer. All other constraints remain the same as those in the PBSSL model.

4. The metaheuristic solution method

The Erlang loss function in equation (1) is highly nonlinear in terms of decision variable s_j ; therefore, we propose a metaheuristic method to search for the quality solutions for PBSSL and JBSSL models. For given station j , the heuristic algorithm is based on an important linear relationship between s_j and θ_j during a battery charging cycle.

4.1. Characterizing the relation between s_j and θ_j

Constraints (25) and (27) in the JBSSL model aim to control the

$$z - \tilde{z} = F_1 + F_b \left(\sum_{i=1}^l \theta_i c + c_0 \right) - \left[F_1 + F_b \left(\sum_{i=1}^n \theta_i c + c_0 \right) + F_2 + F_b \left(\sum_{i=n+1}^l \theta_i c + c_0 \right) \right] \leq 0.$$

stockout probability $B_j(s_j)$ in each station. Note that $B_j(s_j)$ is a monotone decreasing function of s_j ; thus, the optimal solution favors a minimum value of s_j to make (27) either be, or be close to, binding. In other words, for each candidate station, the optimal battery quantity should be close to $s_j^*(\gamma) = \{s_j | B_j(s_j - 1) > \gamma \text{ and } B_j(s_j) \leq \gamma\}$ where γ is the stockout probability.

For a given γ , Fig. 4 reveals the relationship between $s_j^*(\gamma)$ and θ_j

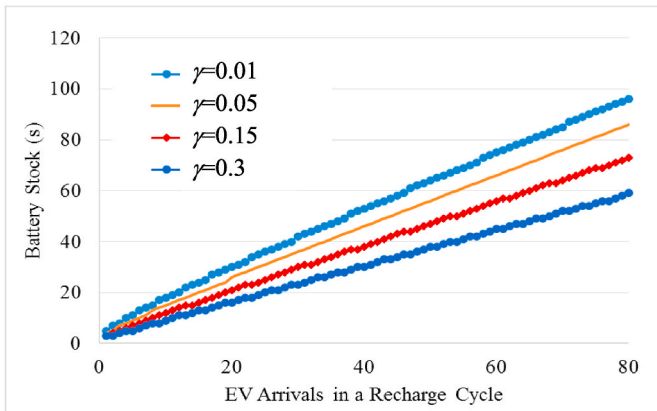


Fig. 4. The Relation between $s_j^*(\gamma)$ and θ_j .

Table 2
Linear regression test results.

γ	Intercept	Slope	p-value	Adjusted R^2
0.01	20.84	1.00681	0.001	0.9996
0.05	11.3751	0.9538	0.001	0.9999
0.15	5.2351	0.8505	0.001	0.9998
0.30	2.64934	0.70016	0.001	0.9999

which is the expected EV arrivals to station j during $1/\mu_b$. It shows that $s_j^*(\gamma)$ and θ_j are almost linear. Table 2 provides justification of the fitness of the linear regression between $s_j^*(\gamma)$ and θ_j as γ varies from 0.01 to 0.3. It suggests that s_j increases linearly with θ_j regardless of γ (i.e. $R^2 \approx 1$). This observation is important as it not only simplifies the nonlinear constraint (27), but also leads to the following theorem and subsequent metaheuristic algorithm.

Theorem 1. For a given stockout probability γ , if the optimal value $s_j^*(\gamma; \theta)$ is a linear function of θ , i.e., $s_j^*(\gamma; \theta) = c(\gamma)\theta + c_0(\gamma)$ for some $c(\gamma), c_0(\gamma) \in \mathbb{R}$, where c and c_0 are linear coefficients for a given γ . Then the optimal location-allocation strategy for the JBSSL model is to assign EV to an existing station instead of opening a new one.

Proof. For a given γ , consider two feasible strategies. The first strategy assigns all customer zones or traffic analysis zones (TAZ) to one JBSS station with the total cost of $z = F_1 + F_b(\sum_{i=1}^l \theta_i c + c_0)$. The second assigns n of the TAZ to one station and assigns the remaining zones to the second JBSS station. Thus, its associated cost is $\tilde{z} = F_1 + F_b(\sum_{i=1}^n \theta_i c + c_0) + F_2 + F_b(\sum_{i=n+1}^l \theta_i c + c_0)$. Hence, we have:

Therefore $z \leq \tilde{z}$.

Theorem 1 suggests an optimal solution should exploit an existing station as much as possible to minimize the number of charging stations opened. We design a metaheuristic algorithm by first determining the maximum arrival rate with which station j can handle, $\bar{\lambda}_j$, subject to the grid power capacity limit P_j .

4.2. Construction of initial feasible solution

One important step in the station location-allocation decision is to convert the power capacity to the number of EV that a station can handle. For a given γ and P_j at station j , the process of converting the power capacity to the largest allowable EV arrival rate is given in Algorithm 1. For the PBSSL model, based on Theorem 1, the algorithm increases the number of spare batteries before it violates the power capacity limit. In the JBSSL model, m is determined in a similar manner. The process repeats by increasing λ_j until the power capacity of station j is violated.

Algorithm 1

$\bar{\lambda}_j = \text{MaxArrival}(P_j, \gamma)$ // the maximal EV arrivals handled by station j

-
1. Initialize station power demand $P = 0$, and $\bar{\lambda}_j = \mu_b$,
 2. Repeat,
 - a. For PBSSL, increase s (from $s = 1$) until W_{\max} is reached using Equation (16)
 - b. For JBSSL model, do the following
Based on the s from previous step, increase m (from $m = 1$) until $\tau_b (1-B_j(s_j)) + W_j \times B_j(s_j) \leq W_{\max}$ (see Equation (27)),
 - c. Update P using Constraint (18) for PBSSL or (29) for JBSSL,
 - d. If the power demand $P \geq P_j$, then terminate;
 - e. $\bar{\lambda}_j = \bar{\lambda}_j + \mu_b$
 3. Return $\bar{\lambda}_j$
-

Algorithm 2

$N_j = \text{MaxZones}(\bar{\lambda}_j)$ // the maximum number of TAZ covered by station j

-
1. Initialize $\lambda_j = 0$
 2. S_j = the set of TAZ that can be covered by station j (i.e., $d_{ij} = 1$), and are sorted by arrival rate λ_i in ascending order. Let i be the index for all TAZ in the ordered set.
 3. For $i = 1$ to $|S_j|$
 $\lambda_j = \lambda_j + \lambda_i^i$
 If $\lambda_j > \bar{\lambda}_j$ then break;
 End for
 4. Return $N_j = i-1$
-

Based on the maximum arrival rate $\bar{\lambda}_j$ for station j , we compute the maximum number of TAZ, denoted as N_j , that can be assigned to station j . This is because constraint (12) requires all TAZ be covered. To minimize the total setup cost, the model opts to open the least number of stations with each serving as many TAZ as possible. Algorithm 2 first sorts all TAZ that can be covered by station j in ascending order of λ_i . It then chooses the first N_j customer zones in the sorted list until the maximum arrival rate $\bar{\lambda}_j$ is reached; thus, N_j is treated as the maximum number of zones covered by station j . Note that the sorted list is used to determine N_j , but not the final assignment of TAZ to station j . The latter is determined by Algorithm 3.

Using the maximum number of TAZ station j can cover, Algorithm 3 actually allocates the TAZ to the station by enumerating all N_j combinations of TAZ and choosing the one that yields the maximum arrival rate for the station.

Algorithm 3

$(\bar{y}_{ij}, \bar{x}_j) = \text{Assign}(N_j, \bar{\lambda}_j)$ // Assignment of TAZ to stations

-
1. Let $T_j^1, T_j^2, \dots, T_j^K$ be K sets of TAZ such that: $|T_j^k| = N_j$ and $d_{ij} = 1$, for all $i \in \{1, \dots, N_j\}$, for all $k = 1, 2, \dots, K$.
 2. Let $\lambda_{j,1}^k, \lambda_{j,2}^k, \dots, \lambda_{j,N_j}^k$ be the arrival rates at all N_j stations in the k -th set.
 3. Let $k^* = \text{argmax}_k \left\{ \sum_{l=1}^{N_j} \lambda_{j,l}^k \mid \sum_{l=1}^{N_j} \lambda_{j,l}^k \leq \bar{\lambda}_j \right\}$
 4. Assign and return $y_{ij} = 1$ for all $i \in T_j^{k^*}$.
-

Once the assignment of TAZ to a candidate station j is completed, the allocation of batteries and superchargers are obtained by Algorithm 4. As mentioned previously, in order to minimize objective function (11) or (24), the least amount of batteries and/or superchargers are preferred so long as the service level constraints (16) and (27) are met. On the other hand, since increasing the spare batteries reduces the supercharger number, it is perhaps advantageous to overachieve service level γ in an effort to reduce m up to 1 as long as constraint (29) is not violated. This is because the cost of installing a supercharger is much more expensive than purchasing a spare battery.

Algorithm 4

$(s_j^*, m_j^*) = \text{Configure}(P_j, \lambda_j, \gamma, \beta)$ // calculate the number of batteries and superchargers at station j

-
1. Repeat
 - a. Increase s (from $s = 1$) and increase m (from $m = 1$) until the equality is met in constraint (27)
 - b. Update power demand P using constraint (29)
 - c. $s_j^* = s, m_j^* = m$ and calculate total cost $z^* = F_b s + F_d m$
 2. Repeat
 - i. Increase battery $s = s + 1$, and calculate m so that constraint (27) is satisfied.
 - ii. Calculate total cost $z' = F_b s + F_d m$ and update P (constraint (29))
 - iii. If $z' < z^*$, then $z^* = z', s_j^* = s$ and $m_j^* = m$
 - iv. If $m = 1$ or $P > P_j$, then terminate;
 3. Return s_j^* and m_j^*
-

Algorithm 5 below integrates Algorithms 1 through 4 to provide a heuristic solution to JBSSL. Note that the solution to PBSSL can be obtained by simply removing those procedures related to determining the optimal number of superchargers from Algorithm 5. Particularly, Algorithm 5 first uses Algorithms 1 and 2 to calculate the maximum number of TAZ that a candidate station can cover, then uses Algorithm 3 to assign TAZ to all opened stations and finally determines the numbers of spare batteries and superchargers for each opened station.

Algorithm 5

A heuristic algorithm for the JBSSL model

-
1. Initialize $I^* = \emptyset, J^* = \emptyset, \text{flag}(j) = \text{false}$ for all j ;
 2. //Open those must-open stations and assign TAZ to them
 - a. Identify those TAZ that can be covered by only one candidate station, i.e.,
 $I^* \leftarrow \{i \mid \exists j : d_{ij} = 1, d_{ij'} = 0 \text{ for all } j' \neq j\}$ and
 $J^* \leftarrow \{j \mid \exists i : d_{ij} = 1, d_{ij'} = 0 \text{ for all } j' \neq j\}$
 - b. Update x_j, y_{ij} and P_j .
 3. While $|I^*| \neq |I|$ do
 - a. If $J^* \neq \emptyset$ then
 - For all $j \in J^*$ and $\text{flag}(j) = \text{true}$
 - i. Calculate $\bar{\lambda}_j = \text{MaxArrival}(P_j, \gamma)$ and $N_j = \text{MaxZones}(\bar{\lambda}_j)$
 - ii. Calculate $(\bar{y}_{ij}, \bar{x}_j) = \text{Assign}(N_j, \bar{\lambda}_j)$
 - iii. Calculate $(s_j^*, m_j^*) = \text{Configure}(\bar{y}_{ij}, \bar{x}_j)$
 - iv. $\text{flag}(j) = \text{true}$ and update I^*
 - EndFor
 - b. If $J^* = \emptyset$ then
 - i. Open a new station with the maximum zones $j^* = \text{argmax}_{j \in J^*} \{N_j\}$. If there is a tie, then the station with the lower setup cost is selected.
 - ii. Update $J^* = J^* \cup j^*$
 - EndIf
 - EndWhile
-

4.3. Tabu search algorithm

Since the queueing constraints in JBSSL are nonlinear, Tabu search is employed to further improve the solution quality. Tabu search (Glover 1986) aims to find the best solution in a defined neighborhood at every iteration in order to escape from local optima. Algorithm 6 uses Tabu search to reassign TAZ to different stations with potential of closing some stations, thus minimizing the total cost. A Tabu list is created to track all historical solutions for higher efficiency. Particularly, we consider two types of neighborhood functions as follows:

- **Substitution:** Randomly select two unopened candidate stations. If the total setup cost of the two is smaller than an opened station, we open these two stations and re-assign TAZ to them and the other opened stations. This is motivated by Algorithm 5 in which the priority is given to stations' maximum zones N_j (see Step 3-b-i), not the setup cost.

- **Move:** Randomly select several TAZ covered by an opened station j . Move them to another opened station so long as the power capacity is not violated. This neighborhood function can reduce the number of batteries required in station j and possibly the total cost.

Note that two hard constraints (27) and (29) in the JBSSL model will be ensured in both neighborhood functions. Particularly W_{\max} in (27) will be used to recalculate s_j for the neighborhood solution, and P_j in (29) will be checked for grid capacity limit. If any violation occurs, the neighborhood solution is discarded.

Algorithm 6

A Tabu search algorithm for global optimization for JBSSL

```

1. Initialize: Set Tabu list  $\Gamma = \emptyset$ , maximum iteration as  $L$ , neighborhood size as  $N$ , iteration index  $l = 1$  and initial solution  $\vec{w} = (\vec{y}_{ij}, \vec{x}_j, \vec{s}_j, \vec{m}_j)$ .
   Set optimal solution as  $w^* = w$  and optimal cost as  $Z^* = Z(w^*)$ .
2. While  $l \leq L$ 
  a. Initialize neighborhood list  $N$ 
  b. While Tabu list  $\Gamma$  is not full and the neighborhood list  $N$  is not full
    i. Randomly choose either the substitution or move neighborhood function to create a new solution  $w'$ .
    ii. If  $w'$  is not on the Tabu list, Then
      1) Add  $w'$  to the neighborhood list.
      2) Calculate the total cost for the neighborhood solution  $w', Z(w')$ .
      3) If  $Z(w') < Z^*$ , then:  $w^* = w'$  and add  $w'$  to the Tabu list.
    EndIf
  EndWhile
  c.  $l=l+1$ 
EndWhile
    
```

4.4. An illustrative example for metaheuristics

We use six TAZ and three candidate station locations to illustrate the implementation of the Tabu algorithm on JBSSL. Table 3 lists the information about d_{ij} , the power capacity and setup cost for candidate stations, and the EV arrival rate of each zone. $W_{\max} = 0.5$ h is set as the required total service time.

First, Algorithm 1 is used to calculate the maximum EV arrivals each candidate location can handle. As a result, $\bar{\lambda}_1 = 17.75, \bar{\lambda}_2 = 16.75$ and $\bar{\lambda}_3 = 20.5$. Next, we apply Algorithms 2 and 3 to calculate the maximum TAZ covered by each station, and find that Station 1 covers TAZ 3, 4, and 6; Station 2 covers 4 and 6; and Station 3 covers 1, 3, and 6. Since Stations 1 and 3 can serve three TAZ while Station 2 has a lower setup cost, we opt to open Station 1 first. Subsequently, we assign TAZ 1, 4, and 6 to Station 1. Next, we need to cover TAZ 2, 3, and 5. Realizing Station 2 is only able to cover TAZ 2 and 5 while Station 3 can cover TAZ 2, 5, and 3, we prefer to open Station 3. Now we start to allocate batteries and superchargers. Station 1 is expected to serve 15 EV/h; therefore by Lemmas 1 and 2, the initial $s_1 = 2$ batteries and $m_1 = 14$ superchargers with the total cost of \$644,000 and total power of 623.68 kW, which corresponds to $W = 0.495$ h. We then keep increasing s_1 until either the power exceeds the capacity or m_1 drops to 1. Finally, among all potential solutions, $s_1 = 32$ and $m_1 = 6$ yield the lowest cost of

Table 3
Data for Customer Zones and Candidate Locations (n/a = not applicable).

TAZ\Station	$j=1$	$j=2$	$j=3$	λ_i (EV/hour)
$i=1$	1	0	1	6
$i=2$	0	1	1	8
$i=3$	1	0	1	3
$i=4$	1	1	0	4
$i=5$	0	1	1	9
$i=6$	1	1	1	5
Power capacity P_j (kW)	700	650	800	n/a
Setup cost F_j (× \$1000)	300	500	450	n/a

Table 4
Network size of five experimental sets.

Set	Number of Locations	Number of TAZ	Ratio
1	5	10	2
2	10	20	2
3	20	50	2.5
4	50	200	4
5	200	1000	5

\$494,000 with 660.30 kW (below the capacity). The actual total service time is $W = 0.48$ hour. The same process is repeated for Station 3. The solution is further improved by applying the Tabu search. Finally, Station 1 has 53 batteries and 3 superchargers, and Station 3 has 57 batteries and 3 superchargers, and the total network cost is \$1.79 million.

5. Numerical experiments

5.1. Experimental setting

In this section more complex networks are used to assess PBSSL and JBSSL models. For each experiment, various operational conditions are considered, including EV arrival rate and service time constraint. We test the algorithm on 50 randomly generated instances with ten instances from each of the five design sets shown in Table 4. Each set has distinct network size in terms of the numbers of locations and TAZ. The ratio is defined as the number of TAZ over the number of candidate locations. The proposed algorithm is coded in Python with NumPy plugin (Zelle 2016). All tests are run on Acer V3-372 T with a 2.3 GHz dual core I5 processor and 8 GB of RAM.

In our experiment, Level-2 chargers are used for recharging swapped batteries and Level-3 is for superchargers. For the 24 kWh battery of Nissan Leaf, the average charging duration is 4 h for the swapped batteries, and 0.5 h for a supercharger. The corresponding charge rates are $\mu_b = 0.25$ battery/hour and $\mu_d = 2$ battery/hour, respectively. Other parameters in the PBSSL and JBSSL models are set as: $F_j \sim U$ (\$200,000, \$500,000), $F_b = \$7,000, F_d = \$45,000, P_j \sim U$ (600 kW, 800 kW), $\lambda_i \sim U$ (1, 2) in the unit of EV/hour, and $d_{ij} \sim U$ [0, 1] with uniformly distributed binary value. Battery swap time is set to $\tau_b = 6$ min. Furthermore, for both PBSSL and JBSSL models, five levels of $W_{\max} \in \{10, 15, 20, 25, 30\}$ mins are investigated.

5.2. Results and discussions of PBSSL model

The PBSSL model is evaluated using the 50 randomly generated instances in Table 4. For $W_{\max} = 10$ min, the infrastructure cost, the station number, and the battery stock level for five test sets are summarized in Table 5. The decimal values are the results of averaging ten instances for each set. As expected, the numbers of required stations and spare batteries increase with the network size. In addition, the required battery per station also increases from 30.8 to 81.59.

Fig. 5 is the boxplot of aggregated EV arrival rate in the stations for Set 4. It is interesting to see that W_{\max} does not affect the aggregate arrival rate in the stations. This is because the aggregated EV arrival rates are dependent on the allotted power capacity as in constraint (18). A station tends to reach the power capacity limit so that a fewer stations

Table 5
Average Result for the PBSSL Model with $W_{\max} = 10$ min.

Set	Network Cost (× \$10 ⁶)	Number of PBSS	Total number of batteries	Batteries per station
1	1.3494	2.5	73.8	30.8
2	1.8196	2.9	133	47.6
3	5.3062	6.4	509.5	79.9
4	12.925	15.7	1276.6	81.4
5	65.4624	78.4	6365.6	81.6

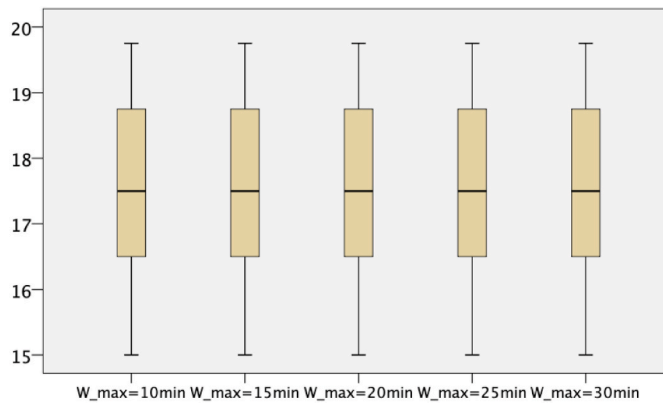


Fig. 5. Aggregated EV arrival rate in station under various W_{max} of PBSSL for Set 4.

Table 6
PBSSL cost (× \$1000) under various W_{max} .

Set	10 mins	15 mins	20 mins	25 mins	30 mins
1	1349.4	1320	1307.4	1296.9	1290.6
2	1819.6	1775.5	1754.5	1743.3	1732.8
3	5306.2	5176.7	5129.8	5087.8	5044.4
4	12925	12603.4	12493.5	12383.6	12273.7
5	65462.4	63860.8	63306.4	62763.2	62214.4

need to open. Thus, the power capacity determines the aggregate EV arrival rates, which is not affected by W_{max} .

Table 6 shows how the total infrastructure cost changes when W_{max} increases from 10 to 30 min. For a given set, the infrastructure cost decreases as W_{max} becomes larger. This is expected because a smaller W_{max} requires more spare batteries. Fig. 6 shows the relative cost changes as W_{max} decreases from 30 to 10 min. The relative cost change is defined as the percentage of the cost increase with respect to the cost at $W_{max} = 30$. For the cost increases linearly as W_{max} decreases from 30 to 15 min. However, the cost jumps up if W_{max} becomes 10 min. That is, when we reduce W_{max} from 30 to 15 min, the cost goes up by approximately 2.5%, but if W_{max} equals 10 min, the cost goes up by about 5%.

Fig. 7 shows the percentage of the battery stock varies with respect to the stock at $W_{max} = 30$ min. The percentage goes up almost linearly across five sets when W_{max} decreases from 30 to 15 min. If W_{max} is further reduced from 15 to 10 min, the percentage of increase doubles. For example, in Set 2 the stock increases only by 5% if W_{max} decreases from 30 to 15 min, but it is 10.2% when W_{max} becomes 10 min.

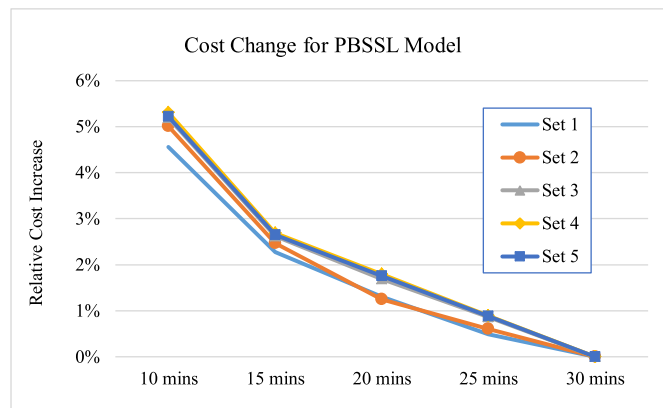


Fig. 6. Percentage of cost change for PBSSL under different W_{max} .

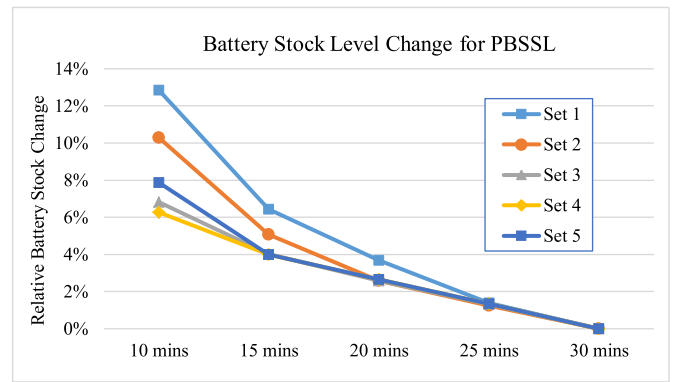


Fig. 7. Percentage of battery stock change for PBSSL under different W_{max} .

5.3. Results and discussions of JBSSL model

The JBSSL model is also tested using the 50 randomly generated instances. Table 7 summarizes the average results for $W_{max} = 10$ min. Three observations can be made. First, as expected, when the network size increases, the infrastructure cost, the battery stock, and the number of opened stations all increase. Second, only one supercharger is needed for each station under $W_{max} = 10$ min. This result shows that the JBSSL model prioritizes the battery swap over supercharge under smaller W_{max} . Third, compared to Table 7, the battery stock for JBSSL is smaller than PBSSL given the same network. For instance, in Set 5 JBSSL requires on average 74.5 battery packs per station as opposed to 81.59 in PBSSL. The reason is because superchargers can substitute certain spare batteries while achieving the same service quality.

5.4. Sensitivity analysis of JBSSL model

Table 8 shows the sensitivity analysis on the JBSSL cost by increasing W_{max} from 10 to 30 min. As expected the total infrastructure cost in each set decreases as W_{max} increases.

Fig. 8 shows how the cost increases as W_{max} decreases from 30 to 10 min with respect to the cost under $W_{max} = 30$ min. The percentage increases almost linearly across five sets for $W_{max} \in [15, 30]$. However, the cost jumps up more rapidly if $W_{max} \in [10, 15]$. For example, in Set 4 the infrastructure cost only increases by 5% as W_{max} decreases to 15 min. However, the cost goes up by more than 10% when W_{max} is down to 10 min. This implies that further reduction of service time from $W_{max} = 15$ min is very costly. Similar observations are also observed in others sets.

Table 9 summarizes the average number of batteries per station under various W_{max} . As expected the battery stock increases across five sets when W_{max} decreases. Fig. 9 shows the percentage of the battery stock changes as W_{max} decreases with respect to the stock for $W_{max} = 30$ min. It shows that the relative stock across five sets goes up almost linearly as W_{max} decreases. This differs from the PBSSL model in Fig. 7

Table 7
Results for JBSSL Model with $W_{max} = 10$ min.

Set	1	2	3	4	5
Number of stations	2.5	2.9	6.4	15.7	78.4
Average cost (× \$1000)	1381.7	1834.6	5286.2	12870.3	65193.6
Total number of batteries	62	116.5	465.5	1167.8	5832.2
Average batteries per station	26.1	41.8	73.03	74.4	74.5
Total number of superchargers	2.5	2.9	6.4	15.7	78.4
Average superchargers per station	1	1	1	1	1
Stockout probability	0.05	0.08	0.06	0.06	0.06
Waiting probability at supercharger	0.23	0.35	0.50	0.51	0.51

Table 8
JBSSL cost (× \$1000) under various W_{max} .

Set	10 min	15 min	20 min	25 min	30 min
1	1381.7	1333.4	1308.9	1293.0	1277.0
2	1834.6	1768.1	1733.2	1709.2	1684.5
3	5286.2	5083.1	4971.8	4883.4	4802.2
4	12870.3	12363.5	12083.7	11869.4	11659.4
5	65193.6	62670.4	61280.0	60182.8	59154.0

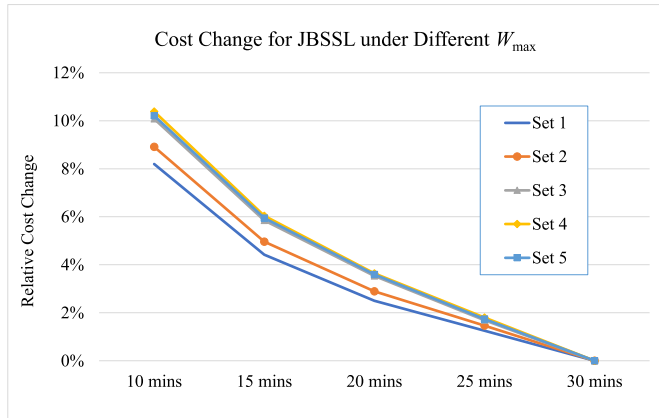


Fig. 8. Percentage of cost change for JBSSL model under different W_{max} .

Table 9
Number of batteries per JBSS station for different W_{max} .

Set	10 min	15 min	20 min	25 min	30 min
1	26.1	23	19.63	17.83	15.41
2	41.8	36.68	32.16	28.24	22.78
3	73.03	61.94	53.74	42.9	31.88
4	74.43	62.94	54.24	44.19	31.94
5	74.32	62.99	54.44	43.56	32.75

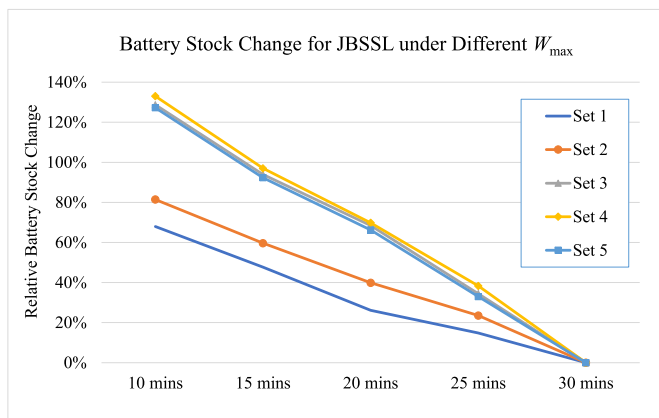


Fig. 9. Percentage of battery stock change for JBSSL model under different W_{max} .

Table 10
Number of superchargers per JBSS station under different W_{max} .

Set	10 min	15 min	20 min	25 min	30 min
1	1	1.05	1.35	1.48	1.71
2	1	1.28	1.7	2.13	2.78
3	1	2.01	2.9	4.28	5.71
4	1	2.07	3.02	4.29	5.89
5	1	2.08	3.13	4.36	5.95

where the cost percentage doubles if W_{max} reaches 10 min compared to $W_{max} \in [15, 30]$. This is a direct benefit of adopting superchargers in the station, so that the amount of spare batteries can be held at a relatively constant level.

Table 10 shows the required superchargers per station under various W_{max} . The number of superchargers decreases as W_{max} reduces. This result seems counter intuitive because a station with more superchargers is supposed to accelerate the service speed. Indeed, the numerical results for the JBSSL model shows that the number of superchargers increases with W_{max} . For example, the number of superchargers increases from 1 to almost 6 in Sets 3, 4 and 5 when W_{max} reaches 30 min. As the current parameter settings pertaining to battery and supercharger, it is more cost effective to use an additional supercharger than it is to use an additional battery. Therefore, when W_{max} increases, the optimal solution tends to reduce the number of batteries and direct EVs to use supercharging bay. Therefore, it requires more superchargers at the station.

5.5. Comparison between tabu and naïve search

To assess the performance of the heuristic algorithm, we solve PBSSL and JBSSL using a Naïve search and the results are used as a benchmark to compare the efficiency of the Tabu search. The Naïve algorithm is presented as Algorithm 7 below. The results of both models are shown in Tables 11 and 12, respectively. For all the instances of PBSSL model, Tabu always yields a lower cost than the Naïve search. The cost saving becomes larger as the network size incases (from Sets 1 to 5). For the JBSSL model, we show the benefit of Tabu search by calculating the percentage of cost reduction. It shows the average cost reduction varies between 5.7 and 6.3% across five sets as W_{max} varies from 10 to 30 min.

Algorithm 7

Naïve algorithm for global optimization for PBSSL and JBSSL

```

Randomly assign each TAZ demand to a station while satisfying power capacity
Initialize BestObj = ∞;
While better solution found
  Loop i in set of TAZ demand
    Create a new random assignment for TAZ demand i to a station j.
  End loop
  1. If the assignment is not exploit previously then calculate number of required
    batteries and superchargers and the new total cost as NewObj
  2. If the new solution is not feasible, then add a large penalty to the NewObj
  3. If newObj < BestObj, update the best solution as BestX
Endwhile
Return BestX
    
```

6. A case study

The JBSSL model is further applied to a central Ohio regional network available at www.morpc.org. The data involves 714,000 households, 2 million light-duty vehicles in seven counties, and 2.5 million personal trips in year 2015. The EV penetration rate is assumed to be 3.3% as suggested in Almeida et al. (2012). Table 13 shows each data entry is a tour consisting of at least one trip. Each trip has designated origin and destination TAZ with known distance. Since the case study focuses on siting charging stations with public accessibility, we choose non-residential areas such as retail stores, shopping malls, office complexes, and gas stations along the highway as candidate locations.

In order to estimate the hourly EV arrival rate λ_i at each TAZ, the number of EV to be charged during its tour is considered. An EV is assumed to be fully charged at the beginning of a tour. Fig. 10a is a box plot for the calculated arrival rates for all TAZ in the case study. The figure suggests that for most TAZ, the hourly arrival rate λ_i is from 1 to 4 vehicles. On the other hand, Kuby and Lim (2005) conclude that about 83.4% of alternative-fuel drivers refill their vehicle when the energy source is less than 3/8 of the full capacity. Therefore, all tours with a

Table 11
PBSSL cost (× \$1000) comparison between Tabu and Naïve search.

Set	10 min		15 min		20 min		25 min		30 min	
	Tabu	Naïve								
1	1349.4	1396.5	1320	1370.6	1307.4	1357.3	1296.9	1344	1290.6	1338.4
2	1819.6	1940.9	1775.5	1905.2	1754.5	1881.4	1743.3	1868.8	1732.8	1857.6
3	5306.2	5787	5176.7	5668	5129.8	5614.8	5087.8	5566.5	5044.4	5523.1
4	12925	13453.7	12603.4	13161.1	12493.5	13035.8	12383.6	12924.5	12273.7	12813.2
5	65462.4	67969.6	63860.8	66513.6	63306.4	65872.4	62763.2	65340.4	62214.4	64786

Table 12
JBSSL cost (× \$1000) under various W_{max} between Tabu and Naïve search.

Set	10 min			20 min			30 min		
	Tabu	Naïve	%	Tabu	Naïve	%	Tabu	Naïve	%
1	1381.7	1430.8	3.6	1308.9	1363.9	4.2	1277	1330.3	4.2
2	1834.6	1973.8	7.6	1733.2	1875.2	8.2	1684.5	1819.7	8.0
3	5286.2	5786.6	9.5	4971.8	5470.1	10.1	4802.2	5297	10.3
4	12870.3	13404.4	4.1	12083.7	12644.2	4.6	11659.4	12217.7	4.8
5	65193.6	67718	3.9	61280	63920.8	4.3	59154	61790.8	4.5
Avg.			5.7%			6.3%			6.3%

Table 13
Sample Data for the Case Study (note: $i, k,$ and l are index for TAZ).

Household No.	Start TAZ i	End TAZ l	Intermediate Stop (TAZ k)	Distance from i to l (km)	Distance from i to k (km)	Distance from k to l (km)
1	1	4		14		
2	14	27	30	19	15	21
3	36	79	45	12	6	7

distance larger than 5/8 of the full battery range could be a potential charge demand at its destination. In fact, an EV battery may have some energy left prior to reaching a station; this buffer is set as 1/8 of the battery capacity. Hence, the maximum allowable range between an EV and its intended charge station is 2/8 of the full battery range. Take the 24 kWh Nissan Leaf battery as the example, its maximum allowable range is 48 km.

The JBSSL model is solved in the central Ohio case under $W_{max}=10$ min. The results in terms of the arrival rates covered by all opened stations, and the number of batteries and superchargers are depicted in Fig. 10b–d, respectively. In particular, two operational scenarios are studied: baseline grid power capacity and doubled power capacity. The model suggests opening 128 stations in the baseline case, which reduces to 60 stations with doubled power capacity. Fig. 10b shows that in the baseline case, the average arrival rate is 18 EV per hour per station. If the power capacity doubles, the average EV arrival rates is approximately 38 cars. In the baseline case, Fig. 10d shows most stations hold 68–80 batteries in stock. When the power capacity doubles, the average battery stock increases to 145 batteries per station. Finally, Fig. 10d shows that only one supercharger is needed per station in the baseline, yet 56 out of 60 stations need at least two superchargers if the power capacity doubles.

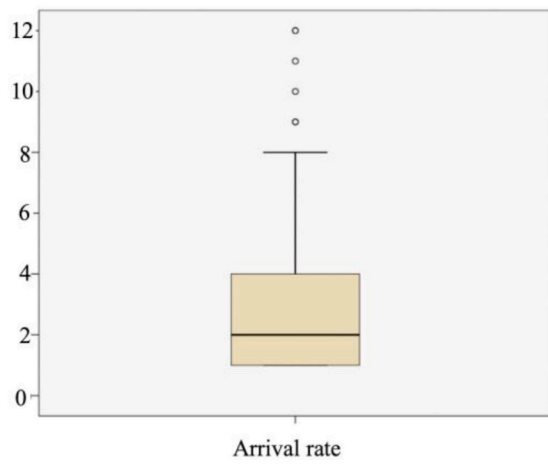
Fig. 11a shows the map of all 128 opened JBSS stations under the baseline power capacity. A darker color represents a higher arrival rate for the TAZ. It shows that most stations are placed in the Columbus metropolitan area (i.e. rectangular box with solid lines). In addition, Fig. 11a marks three example satellite areas (i.e. rectangular boxes with dashed lines) and each contains more stations than its surrounding areas. In particular, the area with the highest EV arrival rates is marked with the star. A zoomed-in view of the Columbus airport is also available in Fig. 11b. The aggregate arrival rate is 124 EV per hour from 27 zones. As a result, seven stations are established as shown in Fig. 11b. These stations are able to meet the demand at 15, 17, 18, 19, 18, 18, and 19 EV/h using 64, 72, 76, 80, 76, 76, and 80 batteries, respectively. Each of

these seven stations have one supercharger installed.

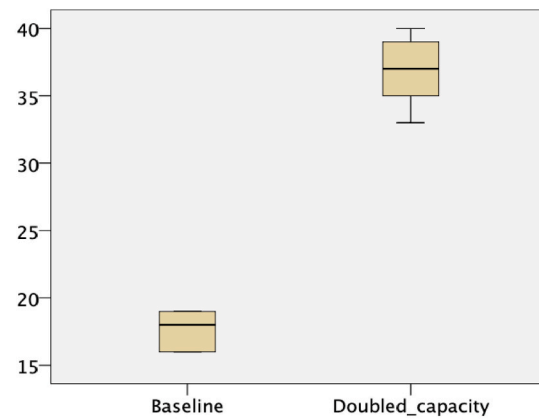
Finally, we increase the charging rate μ_b for charge bay and investigate how it influences the decision on station, spare batteries and superchargers. Table 14 displays the results for $\mu_b = 0.25, 0.5,$ and $1,$ respectively. The following observations can be made. First, increasing μ_b does not influence the number of stations opened, which remains 128. Second, battery stock and supercharges all decrease, as μ_b doubles or quadruples. Third, the total network cost decreases as μ_b doubles or quadruples because a smaller amount of batteries are needed. Finally, when the charging rate is as high as $\mu_b = 1,$ the charging time is so quick that the difference between 20 and 25 min is not enough to cause the network configuration change.

7. Conclusions

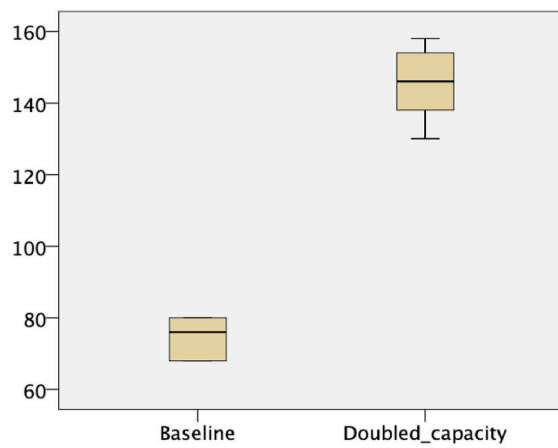
This paper makes an early attempt to propose a location-allocation model for concurrently deploying battery swap and supercharging networks under service time and power grid capacity constraints. The goal is to determine the station site, the battery stock level and the number of superchargers for minimizing the total infrastructure cost. A two-stage priority queue comprised of Erlang B and C is used to control the service quality. The planning model guarantees three performance criteria: battery state-of-charge, total service time, and power grid stability. Several managerial insights are derived based on 50 experimental instances and the case study of the Central Ohio Regional traffic network. First, there exists a critical time threshold. For the 24 kWh battery under study, the network cost for $W_{max} \in [10, 15]$ goes up twice as fast as that under $W_{max} \in [15, 30]$ if the same amount of time is reduced. Second, for a pure battery swap station the battery stock under $W_{max} \in [10, 15]$ increases twice as fast as that under $W_{max} \in [15, 30]$ if the same amount of time decreases. However, for joint battery swap and supercharging the battery stock shows a linear growth rate with the time. Third, if the electric vehicle penetration rate and the network area are fixed, the case study shows the number of opened stations is independent of the



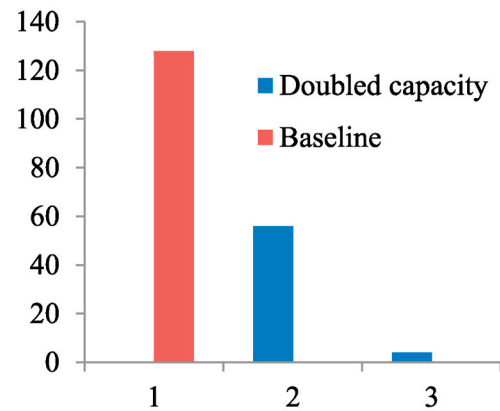
a. Boxplot for arrival rates at TAZ



b. Boxplot for aggregate arrival rate

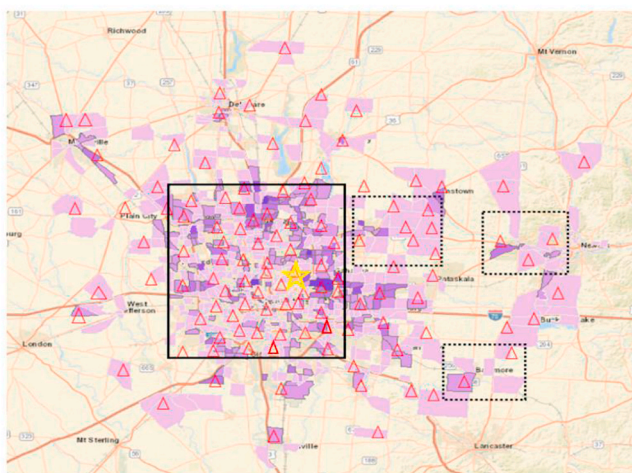


c. Boxplot for number of battery

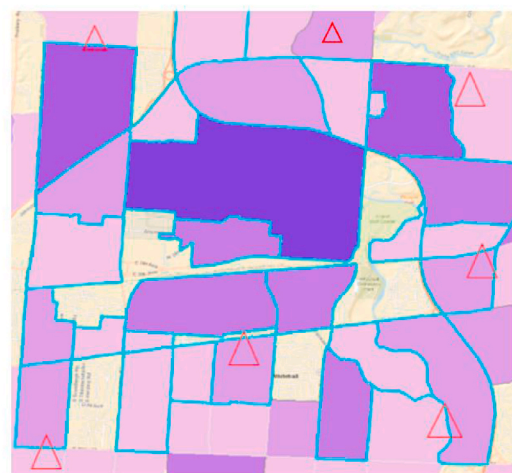


d. Boxplot for installed superchargers

Fig. 10. Results for the central Ohio case.



a. Map of the charging stations for the central Ohio case



b. Zoomed map for charging stations in the Columbus airport area

Fig. 11. Map of the JBSS stations in central Ohio.

Table 14
Results for JBSSL at different charging levels in charge bay (Note: W_{\max} in minutes).

Case	W_{\max}	Stations	Battery Stock	Superchargers	Cost (× \$1000)
Baseline	10	128	73	1	106,876
$\mu_b = 0.25$	15	128	62	2	102,780
EV/h	20	128	53	3	100,492
$P_b = 10$ kW	25	128	44	4	98,792
$\mu_b = 0.5$ EV/h	10	128	39	1	76,832
$P_b = 20$ kW	15	128	38	1	75,068
	20	128	37	1	74,508
	25	128	37	1	74,172
$\mu_b = 1$ EV/h	10	128	22	1	61,376
$P_b = 40$ kW	15	128	21	1	60,228
	20	128	20	1	59,612
	25	128	20	1	59,612

charging power used by charge bay. From transportation management aspect, the proposed service location-allocation models bring together battery swap and onboard supercharging under a unified planning framework. Numerical experiments show that the dual charging mode outperforms a single service mechanism in terms of spare battery stock, service time commitment and power grid stability. From electricity market aspect, this study also facilitates the transition of battery service stations to become a prosumer who not only consumes energy, but also produces electricity. Stations can install wind- and solar-based micro-grid system and participate in the energy market through vehicle-to-grid operation or virtual power plant generation.

Several research directions can be further investigated. For instance, both PBSSL and JBSSL models can be extended and accommodate operational-level decisions by considering battery inventory review policies, vehicle-to-grid operations, and time-varying electricity pricing. In methodology, the mix-integer programming model can be solved by developing cutting plane methods with the piecewise linear approximation technique, and the results can be further compared with the heuristic approach.

Acknowledgement

This research is supported by the US National Science Foundation (NSF) under Division of Chemical, Bioengineering, Environmental, and Transport Systems (CBET) program (grant # 1704933).

References

Almeida, P.M.R., Soares, F.J., Lopes, J.A.P., 2012. Impacts of large-scale deployment of electric vehicles in the electric power system. In: *Electric Vehicle Integration into Modern Power Networks*. New York, NY: Springer, New York, pp. 203–249.

Agassi, S., 2009. World without oil: better place builds a future for electric vehicles (innovations case narrative: better place). *Innovations: Technology, Governance, Globalization* 4 (4), 125–140.

Armstrong, M., El Hajj Moussa, C., Adnot, J., Galli, A., Riviere, P., 2013. Optimal recharging strategy for battery-switch stations for electric vehicles in France. *Energy Pol.* 60, 569–582.

Avci, B., Girotra, K., Netessine, S., 2015. Electric vehicles with a battery switching station: adoption and environmental impact. *Manag. Sci.* 61 (4), 772–794.

Bekker, R., de Bruin, A.M., 2009. Time-dependent analysis for refused admissions in clinical wards. *Ann. Oper. Res.* 178 (1), 45–65.

Bijvank, M., Johansen, S.G., 2012. Periodic review lost-sales inventory models with compound Poisson demand and constant lead times of any length. *Eur. J. Oper. Res.* 220 (1), 106–114.

Byford, S., 2013. Tesla Motors Demonstrates 90-second Model S Battery-Swapping Tech. *The Verge*, June 21. <https://www.theverge.com/2013/6/21/4450664/tesla-mode-l-s-battery-swap-demo>. (Accessed 22 May 2018).

Diabat, A., Dehghani, E., Jabbarzadeh, A., 2017. Incorporating location and inventory decisions into a supply chain design problem with uncertain demands and lead times. *J. Manuf. Syst.* 43, 139–149.

Drezner, Z., Hamacher, H.W., 2001. *Facility Location: Applications and Theory*. Springer Science & Business Media.

Eiselt, H.A., Sandblom, C.-L., 2013. *Decision Analysis, Location Models, and Scheduling Problems*. Springer Science & Business Media.

Fang, S.-C., Ke, B.-R., Chung, C.-Y., 2017. Minimization of construction costs for an all battery-swapping electric-bus transportation system: Comparison with an all plug-in system. *Energies* 10 (7), 890. <https://doi.org/10.3390/en10070890> total 20 pages.

Glover, F., 1986. Future paths for integer programming and links to artificial intelligence. *Comput. Oper. Res.* 13 (5), 533–549.

Jamian, J.J., Mustafa, M.W., Mokhlis, H., Baharudin, M.A., 2014. Simulation study on optimal placement and sizing of battery switching station units using artificial bee colony algorithm. *Int. J. Electr. Power Energy Syst.* 55 (2), 592–601.

Kabli, M., Qaddus, M.A., Nurre, S.G., Marufuzzaman, M., Usher, J.M., 2020. A stochastic programming approach for electric vehicle charging station expansion plans. *Int. J. Prod. Econ.* 220, 107461. <https://doi.org/10.1016/j.ijpe.2019.07.034>.

Kuby, M., Lim, S., 2005. The flow-refueling location problem for alternative-fuel vehicles. *Soc. Econ. Plann. Sci.* 39 (2), 125–145.

Lambert, F., 2017. Tesla Supercharger Network Reaches 1,000 Stations Worldwide and ~7,000 Chargers. *Electrek*, available at: <https://electrek.co/2017/10/03/tesla-supercharger-network-1000-stations/>. (Accessed 24 May 2018).

Li, D., 2016. China's BAIC Group launches EV battery-swap station network in Beijing. *China Money Network*, 2016. <https://www.chinamoneynetwork.com/2016/11/03/chinas-baic-group-launches-ev-battery-swap-station-network-in-beijing> (accessed on June 1, 2018).

Liu, A., Zhao, Y., Meng, X., Zhang, Y., 2020. A three-phase fuzzy multi-criteria decision model for charging station location of the sharing electric vehicle. *Int. J. Prod. Econ.* 225, 107572.

Liu, L., Kulkarni, V.G., 2008. Balking and reneging in m/g/s systems exact analysis and approximations. *Probab. Eng. Inf. Sci.* 22 (3), 355–371.

Liu, N., Chen, Q., Lu, X., Liu, J., Zhang, J., 2015. A charging strategy for PV-based battery switch stations considering service availability and self-consumption of PV energy. *IEEE Trans. Ind. Electron.* 62 (8), 4878–4889.

Mak, H.-Y., Rong, Y., Shen, Z.-J.M., 2013. Infrastructure planning for electric vehicles with battery swapping. *Manag. Sci.* 59 (7), 1557–1575.

Mak, Ho-Yin, Shen, Zuo-Jun Max, 2009. A two-echelon inventory-location problem with service considerations. *Nav. Res. Logist.* 56 (8), 730–744.

Pan, F., Bent, R., Berscheid, A., Izraelevitz, D., 2010. Locating PHEV exchange stations in V2G. In: *Proceedings of First IEEE International Conference on Smart Grid Communications*, pp. 173–178.

Raviv, T., 2012. The battery switching station scheduling problem. *Oper. Res. Lett.* 40 (6), 546–550.

Ren, S., Luo, F., Lin, L., Hsu, S.-C., Li, X.I., 2019. A novel dynamic pricing scheme for a large-scale electric vehicle sharing network considering vehicle relocation and vehicle-grid-integration. *Int. J. Prod. Econ.* 218, 339–351.

SAE, 2010. SAE Electric Vehicle and Plug in Hybrid Electric Vehicle Conductive Charge Coupler J1772_201001. https://www.sae.org/standards/content/j1772_201001/. (Accessed 6 June 2018).

Shen, Z.-J.M., Qi, L., 2007. Incorporating inventory and routing costs in strategic location models. *Eur. J. Oper. Res.* 179 (2), 372–389.

Tan, X., Sun, B., Wu, Y., Tsang, D., 2018. Asymptotic performance evaluation of battery-swapping and charging station for electric vehicles. *Perform. Eval.* 119 (3), 43–57.

Tran, T.H., Nagy, G., Nguyen, T.B.T., Wassan, N.A., 2018. An efficient heuristic algorithm for the alternative-fuel station location problem. *Eur. J. Oper. Res.* 269 (1), 159–170.

Voelcker, J., 2018. 2018 Nissan Leaf Electric Car Gets 151-mile EPA Range Rating. *Green Car Reports*, January, 27. https://www.greencarreports.com/news/1115028_2018-nissan-leaf-electric-car-gets-151-mile-epa-range-rating. (Accessed 22 May 2018).

Wang, Y.-W., Lin, C.-C., 2009. Locating road-vehicle refueling stations. *Transport. Res. E Logist. Transport. Rev.* 45 (5), 821–829.

Whitt, W., 1992. Understanding the efficiency of multi-server service systems. *Manag. Sci.* 38 (5), 708–723.

Widrick, R.S., Nurre, S.G., Robbins, M.J., 2016. Optimal policies for the management of an electric vehicle battery swap station. *Transport. Sci.* 52 (1), 59–79.

Wikipedia, 2020. Tesla Supercharger available at: https://en.wikipedia.org/wiki/Tesla_Supercharger. (Accessed 10 February 2020).

Winston, W.L., 2004. *Operations Research: Application and Algorithms* (Chapter 20). The Fourth Edition, Cengage Learning, Belmont, CA, USA.

Yudai, H., Osamu, K., 2009. A safety stock problem in battery switch stations for electric vehicles. In: *Proceedings of the Eighth International Symposium on Operations Research and its Applications (ISORA09)*, pp. 332–339.

Zelle, J., 2016. *Python Programming: an Introduction to Computer Science*, third ed. (Franklin, Beedle & Associates, Portland, OR, USA).

Zeng, G., 2003. Two common properties of the Erlang-B function, Erlang-C function, and Engset blocking function. *Math. Comput. Model.* 37 (12–13), 1287–1296.